

LUNAR IRON AND TITANIUM DISTRIBUTIONS FOR LQ-4 REGION Zongcheng Ling¹, Jiang Zhang¹, Jianzhong Liu² ¹School of Space Science and Physics and Shandong Provincial Key Laboratory of Optical Astronomy & Solar-Terrestrial Environment, Shandong University, Weihai, Shandong 264209, P. R. China; ²Institute of Geochemistry, Chinese Academy of Sciences, Guiyang 550002, P.R. China, (zcling@sdu.edu.cn)

Introduction:

Imaging Interferometer (IIM) is the first Chinese lunar imaging spectrometer aboard Chang'E-1, with the science goal to detect the lunar chemical and mineralogical compositions [1,2]. Unlike other recently lunar imaging spectrometers, e.g., Moon Mineralogy Mapper and Multiband Imager [3-4], IIM is a Fourier transform Sagnac-based imaging spectrometer. Detailed parameters can be found in the reference [5-6]. Until now, many achievements have been made with the application of IIM data including elemental mapping as well as data calibrations [5-9]. Iron (FeO) and titanium (TiO₂) are two important elements for the moon. Their distribution and abundance across the moon will provide key information for the petrogenesis of lunar rocks and the thermal history of the Moon [10-14]. We have obtained two new preliminary models for mapping FeO and TiO₂ by using IIM data [5,6]. Here we will present our new models of iron and titanium mapping based on newly calibrated data set.

IIM data:

IIM operates from visible to near infrared (0.48-0.96 μm) with 32 spectral channels. When on a polar orbit of 200 km above the Moon, Chang'E-1 IIM yields a ground resolution of 200m/pixel and 25.6 km swath width. The IIM data processing pipeline include dark current subtraction, relative calibration, spectrum reconstruction, radiometric calibration, photometric normalization and reflectance conversion, etc.

As the first interference spectrometer targeted for the Moon, the processing and calibrations of IIM data are somewhat immature. We have conducted calibration procedures like the flat-field (nonuniformity) correction, spectral calibration (cross-calibration based on telescopic data), distance correction, etc, in order to improve the data quality. IIM data used in this paper is based on the above calibration procedures.

Algorithms to derive FeO and TiO₂ contents:

The preliminary methods for calculating the FeO and TiO₂ abundances have been shown in Ref. 5 and 6. In the new models, we carefully chose and located the available 38 Apollo and Luna landing sites from IIM data. Typically, we average 2X2 pixels for the landing sites with intent to lower the data noise for the input parameters of our models.

For the mapping of FeO, the key is in calculations to suppress the maturity effect by an angle named Fe sensitive parameter θ_{Fe} , which would have a linear relationship with FeO abundance [13]. We obtained the origin at (0.037, 1.351), which yields a coefficient of determination (R^2) of 0.95721.

We got formula to calculate FeO as follows,

$$\theta_{\text{Fe}} = -\arctan\left(\frac{R_{891}/R_{757} - 1.351}{R_{757} - 0.037}\right)$$

$$\text{wt.\% FeO} = \theta_{\text{Fe}}^2 \times 54.775 + \theta_{\text{Fe}} \times 99.142 + 49.597$$

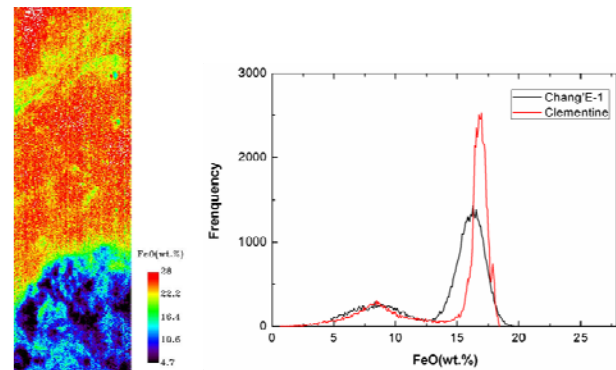


Fig.1. FeO map near the southern rim of Mare Crisium and its data distribution in comparison with that of Clementine UV-VIS.

Figure 1 shows the FeO map near the southern rim of Mare Crisium and its data distribution in comparison with that of Clementine UVVIS. The new FeO model shows an obvious improvement compared to that of Ref. 5. The shift of the low FeO region (as shown in Figure 4 of Ref. 5) has been corrected by this formula. However, for the Hi-Fe endmember, it seems still have a small underestimation of about 0.5 wt. %.

Similarly, we derived the algorithm of TiO₂ by using the Ti-sensitive parameter θ_{Ti} , which would have a power-law relationship with TiO₂ abundance [13]. By maximizing the quality of the second-order polynomial fit between remotely-measured θ_{Ti} and TiO₂ contents, we got the origin at (0.076, 0.573), which yields a coefficient of determination (R^2) of 0.85096.

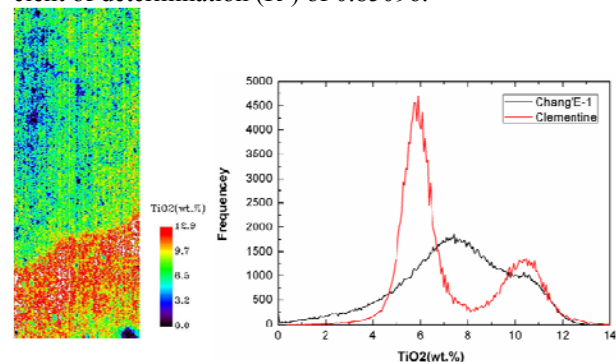


Fig.2. TiO₂ map near MS2 mare region and its data distribution in comparison with that of Clementine UVVIS.

We got the expression of θ_{Ti} as

$$\theta_{\text{Ti}} = \arctan\left(\frac{R_{522}/R_{757} - 0.573}{R_{757} - 0.076}\right)$$

The equation of best fit for TiO_2 mapping is

$$\text{wt.\%TiO}_2 = 0.511 \times (\theta_n)^{7.158}$$

Figure 2 shows the TiO_2 map near MS2 mare region and its data distribution in comparison with that of Clementine UVVIS. The high-titanium mare basalt matches well. While for the low-Ti endmember, our model still show an overestimate $\sim 1.5\text{wt.\%}$. This is mainly due to the fact that IIM data did not cover Apollo 15 landing site, thus leading to the lack of low-Ti basalt as input parameters. In addition, the relatively poor quality of IIM data (lower SNR) will also lead to the broadening of the low-Ti peak as well as that of High-Fe peak (as shown in Figure 1).

FeO and TiO_2 images for LQ-4 region:

By using these two formula, we applied them to the mapping of FeO and TiO_2 for LQ-4 region ($0^\circ\text{--}60^\circ\text{W}$, $30^\circ\text{--}65^\circ\text{N}$). There are many impact basins in LQ-4 region, e.g., the Oceanus Procellarum, Mare Imbrium, Mare Frigoris, etc. Especially, the Sinus Iridium, which would be the target landing site for Chinese Chang'E-3 (with a lander and a rover), is also included in LQ-4. This mosaic was produced by using 114 orbits of IIM datasets from orbit No.230 to No.2909.

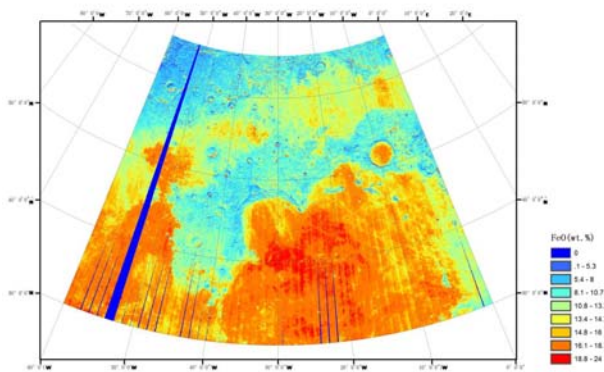


Fig. 3. Mapping FeO abundance for LQ-4 region by using Chang'E-1 IIM data. The image is in Lambert Conform Conic projection

As shown in Figure 3, LQ-4 includes a variety of highland and mare basalt geological units. FeO contents vary abruptly, which make it useful to estimate the boundary between highland and mare regions. Generally, the FeO abundance for highland is less than 10 wt.%, while the FeO content in mare is always beyond 11 wt.%. FeO for the highland region between Mare Frigoris and Mare Imbrium seems to be contaminated with more iron rich basaltic materials, owing to the impact processes which bring ejecta from nearby mare regions.

Figure 4 shows the distribution of TiO_2 across LQ-4 region. As is known, TiO_2 could be regarded as a marker for classification of lunar mare basalts due to its large variations in values. As shown in the Figure 4, the TiO_2 content for high-Ti regions are beyond 9wt.% in the

central Imbrium and northeastern Oceanus Procellarum. They were regarded as younger Eratosthenian basalts[15]. The inner Sinus Iridium and northwestern Oceanus Procellarum and north eastern Imbrium is with medium TiO_2 content ($6\text{wt.\%} < \text{TiO}_2 < 9\text{wt.\%}$). However, the lunar basalts in Mare Frigoris vary from low-Ti to very low-Ti basalt (less than 4wt.%), corresponding to the late Imbrian period between 3.4 and 3.8 Gyr ago[16]. Note that the basalt in Sinus Iridium varies from high-Ti to very low Ti in composition, in-situ detection of these mare basalt by Chang'E-3 rover would be of great interest and significance to reveal distinct lava flows and their formation histories.

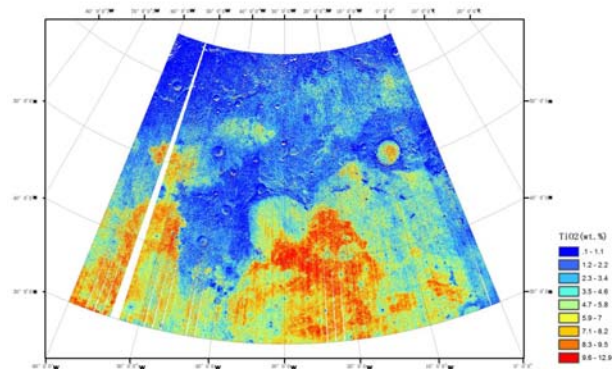


Fig. 4. Mapping TiO_2 abundance for LQ-4 region by using Chang'E-1 IIM data. The image is in Lambert Conform Conic projection

Conclusions and future work:

We have obtained new FeO and TiO_2 models by using the IIM data. In comparisons with Clementine UVVIS results and previous studies, our new FeO and TiO_2 algorithms show obvious improvements, although its constraints due to the lack of Apollo 15 data should not be neglected. We also produced FeO and TiO_2 maps for LQ-4 region, which might be of great potential utilizations for lunar geologic studies by using IIM data.

Acknowledgements: This work was supported by the National Natural Science Foundation of China (No. 11003012, No. U1231103), the Natural Science Foundation of Shandong Province (No. ZR2011AQ001).

References: [1].Zheng,et al.(2008) Planet. Space Sci., 56, 881-886. [2] Ouyang et al.(2010) Chin. J. Space Sci., 2010, 30(5), 392-403. [3] Pieters et al.(2009), Current Science. 96, 500-505. [4].Ohtake et al., (2010) Space Sci. Rev. 154: 57-77 [5].Ling et al.,(2011) Chin. Sci Bull., 56(4-5), 376-379. [6] Ling et al.,(2011) Chin. Sci. Bull., 56(20), 2082-2087. [7] Liu et al., (2010), Sci. China Phys. Mech Astron. 53(12), 2136-2144. [8]. Wu et al.(2010), Planet Space Sci, 58, 1922-1931. [9]. Wu et al.,(2012) JGR. 117, E02001. [10]. Lucey et al. (1995) Science, 268, 1150-1153. [11] Blewett et al.(1997) JGR, 102, 16319-16325. [12] Lucey et al. (1998) JGR,103, 3679-3699. [13] Lucey et al. (2000) JGR, 105, 20297-20305. [14] Wilcox et al. (2005) JGR, 110, E11001.[15].Hiesinger et al.(2000), JGR, 105, 29239-29275. [16].Hiesinger et al.(2010),JGR,115, E03003.